

Article

# Exploring the Dynamic Behavior of Crude Oil Prices in Times of Crisis: Quantifying the Aftershock Sequence of the COVID-19 Pandemic

Fotios M. Siokis

School of Economics and Regional Studies, University of Macedonia, 546 36 Thessaloniki, Greece; fsiokis@uom.edu.gr; Tel.: +30-2310-891-459

**Abstract:** Crude oil prices crashed and dropped into negative territory at the onset of the COVID-19 pandemic. This extreme event triggered a series of great-magnitude aftershocks. We seek to investigate the cascading dynamics and the characteristics of the series immediately following the oil market crash. Utilizing a robust method named the Omori law, we quantify the correlations of these events. This research presents empirical regularity concerning the number of times that the absolute value of the percentage change in the oil index exceeds a given threshold value. During the COVID-19 crisis, the West Texas Intermediate (WTI) oil prices exhibit greater volatility compared to the Brent oil prices, with higher relaxation values at all threshold levels. This indicates that larger aftershocks decay more rapidly, and the period of turbulence for the WTI is shorter than that of Brent and the stock market indices. We also demonstrate that the power law's exponent value increases with the threshold value's magnitude. By proposing this alternative method of modeling extreme events, we add to the current body of literature, and the findings demonstrate its practical use for decision-making authorities—particularly financial traders who model high-volatility products like derivatives.

**Keywords:** dynamical scaling behavior; complex systems; system modeling; power law; energy; financial crises

**MSC:** 37M10; 91G15; 91B82



**Citation:** Siokis, F.M. Exploring the Dynamic Behavior of Crude Oil Prices in Times of Crisis: Quantifying the Aftershock Sequence of the COVID-19 Pandemic. *Mathematics* **2024**, *12*, 2743. <https://doi.org/10.3390/math12172743>

Academic Editors: Alejandro Ramírez-Rojas and José Rubén Luevano Enríquez

Received: 5 August 2024

Revised: 30 August 2024

Accepted: 2 September 2024

Published: 3 September 2024



**Copyright:** © 2024 by the author. Licensee MDPI, Basel, Switzerland. This article is an open access article distributed under the terms and conditions of the Creative Commons Attribution (CC BY) license (<https://creativecommons.org/licenses/by/4.0/>).

## 1. Introduction

The recent public health crisis, apart from causing human destruction, has had enormous effects on the global financial markets, inducing one of the worst crises since the Great Depression. Immediately after the World Health Organization declared the public health crisis as a pandemic, on 11 March 2020, many countries imposed strict lockdowns and quarantines in an effort to contain the spread of the virus. The effects of the pandemic were immediate and devastating, causing a state of paralysis in economic activity and triggering a severe decline in stock market prices, bonds and commodity prices. Among the commodities, the price of the WTI, a benchmark of crude oil, became negative for the first time in history at the onset of the COVID-19 crisis, with the implementation of the lockdown, as efforts to contain the spread of the virus intensified. In particular, on 20 April 2020, the price of the WTI saw a decrease of 302%, settling at USD −37.63 per barrel, from USD 18.31 the day before. As the supply of oil remained at very high levels, thanks to a disagreement between Saudi Arabia—the largest producer of oil—and Russia, while there was a steep decline in the global demand and an increase in oil inventories, traders in the futures market, fearing that the storage capacity would be depleted, paid USD 37.63 per barrel on this particular day just to dispose of their futures contracts. The very next day, the price of Brent, the other well-known benchmark of crude oil, fell to its lowest level ever of USD 9.12 per barrel, from USD 17.36 per barrel the previous day. This change constituted a decrease in price of 47.5%.

Summarizing, the crude oil market suffered simultaneously from two different and significant shocks: one coming from the supply side, as tensions caused an increase in the quantity supplied, and the other from the demand side, as the health pandemic and consequently the lockdown abruptly and drastically decreased the quantity demanded.

Understanding that crude oil is used as a raw material for the production of goods and services, any large fluctuations and turbulence in oil prices impact immediately the production of goods, triggering significant changes in prices, and could have adverse consequences for the real economy. It is therefore of great interest, particularly for decision-making authorities, academics and corporate managers, to analyze sudden changes in oil prices and their impacts on the economy and the cost of raw materials used in the production process. This is especially relevant in the context of the COVID-19 pandemic, which has caused oil prices to deviate significantly from their normal trajectory.

In this study, we propose a novel methodology to model the behavior of oil prices during periods of extreme events. We examine the dynamics of crude oil prices, along with other stock market indices, under distress conditions; more specifically, we analyze the statistical properties of the time series immediately following the occurrence of a major shock to the price of crude oil. The focus is on the distribution of rare events, since a complex system's statistical characteristics are better revealed during times of severe distress [1] (Johansen and Sornette, 1998). Our primary objective is to contribute to the existing literature, which was initiated by [2] (Lillo and Mantegna, 2004), who primarily focused on evaluating the stock market volatility using one-minute time intervals. By expanding upon this research, we aspire to enhance our capacity to predict future market crises and gain a more profound understanding of the underlying complexities of the crude oil market, ultimately benefiting decision-makers, investors and regulators.

The methodology employed is based on the Omori law, established in [3] by Omori (1894); it is a well-known law in seismicity that describes the decay in the rate of aftershocks following a main event. Scaling laws exhibit excellent inheritance and aggregation properties [4] (Gabaix, X., 2009) and have been used in numerous scientific areas in revealing and understanding the distinct characteristics of the data generating process, like correlations, or the underlying regularity in the properties of a particular system. Hence, they could help to impose discipline in theory formation [5]. The behavior of crude oil price changes directly after a major event could be comparable to what occurs in geophysics—specifically, the aftershock sequence that follows a main earthquake. As in earthquakes, large fluctuations in financial prices occur in clusters within a small time interval. The largest fluctuation (typically exceeding the sampling standard deviation multiple times in magnitude) is referred to as the mainshock, while the smaller shocks occurring immediately after the mainshock are called aftershocks.

We contribute to the existing literature by testing the crude oil market following a major shock. This is the first attempt to model the crude oil market with the use of an alternative technique such as the Omori law process. By using relatively high-frequency data, we discover that the aftershock series in the oil commodity markets adhere to a statistical law—specifically, a time power law relaxation process. Our findings are consistent with those observed in stock markets by [2,6] (Weber et al., 2007), indicating a similar pattern of perturbation–response dynamics in daily volatility. This contribution not only deepens our understanding of the crude oil market but also highlights the potential of the Omori law process as a valuable tool for the analysis of complex systems.

The remainder of this paper is organized as follows. Section 2 reviews the literature on the implementation of the power law, particularly in financial crashes, and the characteristics of the aftershock generation process. Section 3 briefly presents the Omori law framework and the data. The main empirical results and the Bath law are discussed in Section 4, while Section 5 presents the policy implications. We conclude in Section 6 and provide future research questions.

## 2. Literature Review

Complex and nonlinear systems and market crashes are modeled as self-organizing hierarchical structures [7–10], in a dynamical out-of-equilibrium system [1,11], exhibiting scale-invariant behaviors.

Power laws have been utilized in other areas besides geophysics, such as in internet traffic and in theoretical economics, and, most importantly, empirical power laws have been utilized in establishing patterns involving cities, firms, the distribution of income and even stock markets [12] (For an excellent survey of power laws in economics and finance, see Gabaix [13]). The Pareto distribution or Zipf's law is one of the most well-known power laws (when the probability of measuring a particular value of some quantity varies inversely as the power of that value) [14].

In geophysics, the Omori law has been tested a number of times and it still attracts considerable attention. Abe et al. [15,16] presented a theoretical approach to describing the Omori–Utsu law for earthquake aftershock sequences, while refs. [17,18] used the modified Omori law to analyze the aftershock hazards, the rate and the duration. In [19], the authors found that the aftershock rate was a critical factor controlling long-term memory, and ref. [20] applied the inverse Omori law, which characterizes the accelerating rate of foreshocks. Furthermore, refs. [21,22] tested the validity of the Omori law along with the Gutenberg–Richter law, and ref. [23] found that the exponents of the two laws were correlated.

In financial markets, Sornette et al. [24] studied the S&P 500 Index before and after Black Monday, i.e., 19 October 1987, and found that the implied market volatility was governed by a log-periodic power law. Lillo and Mantegna [2] examined the aftershock periods of the U.S. stock markets following the occurrence of rare events, particularly the aforementioned Black Monday in 1987. Using one-minute data for a period of 60 trading days, they showed that there was nonlinear activity and the aftershock sequence was well described by a power law function. Di Mateo et al. [25] analyzed the scaling properties of the  $q$ -order moments for a number of different stock exchange indices with the use of the Hurst exponent. They concluded that the Hurst exponent, as a useful instrument, is sensitive to the degree of market development.

Utilizing data from a number of emerging stock markets, ref. [5] revealed that financial volatility is well described by a scaling law, such as the Omori law. In the same vein, ref. [6] found that Omori processes exist in aftershock periods but also in smaller, less significant shocks, and they also can occur on different scales within the same period. The authors in [26] examined the dynamic behavior of Chinese SSEC volatility after large shocks based on daily and one-minute data. They concluded that the aftershock sequence increases as a power law, with the scaling  $p$ -value being an increasing function of the threshold value. However, they noted that the  $p$ -values were significantly greater than 1, which was an outcome of the idiosyncratic microstructure of the Chinese stock market and the heavy government intervention in the market.

Petersen et al. [27] studied the cascading dynamics immediately before and after 219 stock market shocks. By using the Omori law and the Bath law, they found quantitative relations between the mainshock and the parameters quantifying the decay of the foreshocks and aftershocks. Another finding of the study was that stocks with a greater trading volume reacted more quickly and strongly to a market shock than those stocks with a smaller trading volume. Regarding foreign exchange markets, ref. [28] examined the 1997 exchange rate crisis in Southeast Asia. The author applied the Omori law and investigated the foreshocks and aftershocks of numerous currencies after the depreciation of the Thai Baht. A comparison between the foreshocks and aftershocks revealed a different crash magnitude–frequency distribution between countries.

More recently, ref. [29] studied the effect of socioeconomic and political news on a number of financial systems that were significantly impacted by the COVID-19 crisis. They concluded, among other findings, that the financial markets heterogeneously reacted to the pandemic news with different foreshock and aftershock behavior. They also found

that the aftershock relaxation process was faster than the foreshock one. In addition, ref. [30], through the lens of a stylized agent-based market model, quantified the financial market efficiency in processing SARS-CoV-2-related news by means of the observed Omori power law exponents. Along with the Omori law, ref. [31] tested the validity of the Gutenberg–Richter law for a number of stock exchange indices, as well for a number of firm stocks, for the 1987, 2008 and COVID-19 crises. In terms of the comparison between COVID-19 and the financial crisis of 2008, they concluded that the effect of COVID-19 will not last as long as the financial crisis of 2008 and the number of aftershocks does not necessarily decay with time; hence, it does not obey Omori's power law, but rather a generalized Pareto distribution.

Finally, power law relaxation has been predicted and experimentally observed in cities' growth and populations [32–37], solar flares [38], fraud detection in epidemiology [39] and COVID-19 case figures, avalanche models [40], internet traffic [41] and acoustics emissions [42,43].

### 3. Methodology and Data

We use an alternative approach to modeling oil price behavior and analyze the market dynamics and the rate of decay in the oil prices following the mainshock at the beginning of the COVID-19 crisis. We quantitatively describe the time series of crude oil by examining the number of times that the price change in absolute terms exceeds a given threshold value in the nonstationary time period. This study adopts the Omori law (1894), which, in geophysics, describes the properties of aftershocks following significant earthquakes. It states that, after the main earthquake, the aftershock sequence decreases hyperbolically with time, in the order of  $t^{-1}$ , or, alternatively, that the number of aftershocks per unit time decays with a power law, i.e.,  $n(t) \propto t^{-p}$ , where  $t$  is the time since the occurrence of the mainshock. Numerous studies in seismology have estimated the relaxation value ( $p$ ) to be in the interval of 0.8 and 1.2. In 1961, Utsu [44,45] generalized the law, resulting in the following modified Omori Law form:

$$n(t) = \frac{K}{(t+c)^p} \quad (1)$$

where  $n$  is the frequency of aftershocks,  $K$  and  $c$  are constants varying with each sequence to be determined by the data and  $p$  is the decay parameter. According to Lillo and Mantegna (2003) [2], by integrating Equation (1) between 0 and  $t$ , the cumulative number of aftershocks between the mainshock and the time  $t$  can be described.

When  $p \neq 1$ ,

$$N(t) = K[(t+c)^{1-p} - c^{1-p}]/(1-p), \quad (2)$$

and, when  $p = 1$ ,

$$N(t) = K \ln(t/c + 1). \quad (3)$$

Please note that because  $N(t)$  is related to  $n(t)$  by summation, the volatility in  $N(t)$  is much reduced when compared to the fluctuation in  $n(t)$ . Therefore, the measurement of  $N(t)$  yields a more accurate definition of the aftershock duration than does  $n(t)$ .

We examine the dynamics of the WTI and Brent oil prices along with two major stock market indices, namely the Dow Jones Industrial Average (DJIA) and the S&P 500, mainly for comparison purposes. We define the aftershock sequences as the period of 70 days immediately following the occurrence of the mainshock. Specifically, for the WTI, the data range from 21 April 2020 to 29 July 2020, and, for Brent, they range from 22 April 2020 to 30 July 2020 (Please bear in mind that since the Brent mainshock occurred one day after the WTI's, the aftershock sequences (time ranges) for both crude oil prices differ by one day. This discrepancy does not pose any comparison concerns by any means, because the focus is on the value of the  $p$ -exponent. In many disciplines, including finance and especially in geophysics, there is a comparison of the  $p$ -value over a catalog of large-magnitude earthquakes). For the stock market indices, both aftershock sequences start

from 17 March 2020 and end on 24 June 2020. Our main focus is on the COVID-19 period, and, for comparison purposes, we also analyze the global financial crisis.

The data consist of daily closing prices for all indices. The data for crude oil are provided by the U.S. Energy Information Administration [46], while the data for the stock market indices are taken from Bloomberg. Given the price levels of all indices, we first calculate the percentage change in the prices (daily return) as provided by Equation (4):

$$r_{i,t} = \ln(p_{i,t}/p_{i,t-1}) = \ln p_{i,t} - \ln p_{i,t-1} \tag{4}$$

where  $p$  is the index and  $r$  is the rate of return.

Figure 1 illustrates the price level evolution of all indices and the absolute values of the daily percentage rate from 4 January 2000 to 27 February 2022. We have included a longer time period to highlight the significant declines in the WTI prices during the COVID-19 pandemic and the Great Recession. Additionally, the absolute daily percentage rate of the time series demonstrates the substantial impact of the COVID-19 period, particularly on the WTI oil price (302%). In Figure 2, we also display the aftershock sequences in absolute values during the COVID-19 period, which covers the 70 days immediately following the mainshock. The rate of decay for the aftershocks over time is highly pronounced, especially for the WTI, with the larger shocks in terms of magnitude being closer to the mainshock. Table 1 presents the statistical properties of all indices for the two crises. In the COVID-19 sample, the standard deviation for the WTI and Brent shows significantly higher variability compared to the other indices. When comparing the two crude oil indices, the average price change is greater for Brent (2.9%) than for the WTI (0.9%), but the price volatility is larger and more than double for the WTI. The two stock market prices have nearly identical descriptive statistics, which are much lower than those obtained from the oil market. It is important to note that both oil indices exhibit excess skewness and kurtosis in terms of price changes, indicating that the price returns are not normally distributed. Additionally, the WTI demonstrates negative skewness, with a longer left tail in the probability density function. In Table 2, we present the dates of the mainshocks, along with their magnitudes and relative values.

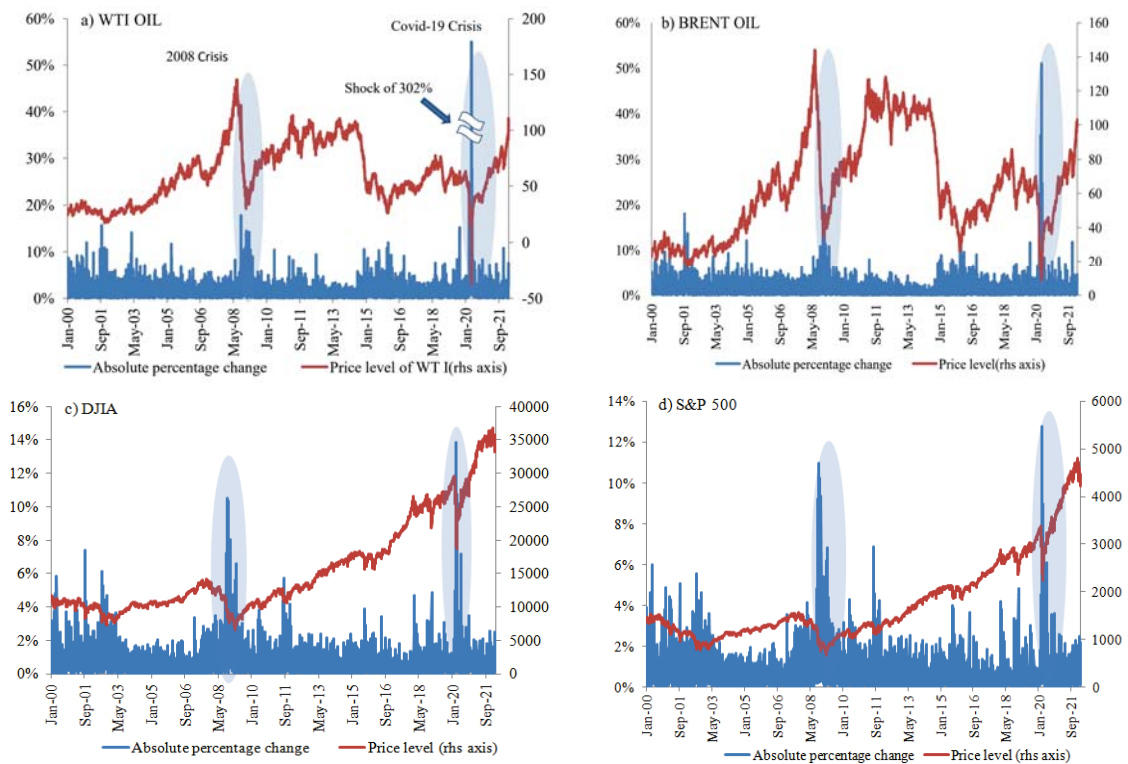


**Figure 1.** Evolution of indices and percentage changes (in absolute terms) for WTI, Brent, DJIA and S&P 500. The shaded areas are the examined periods of the two crises.

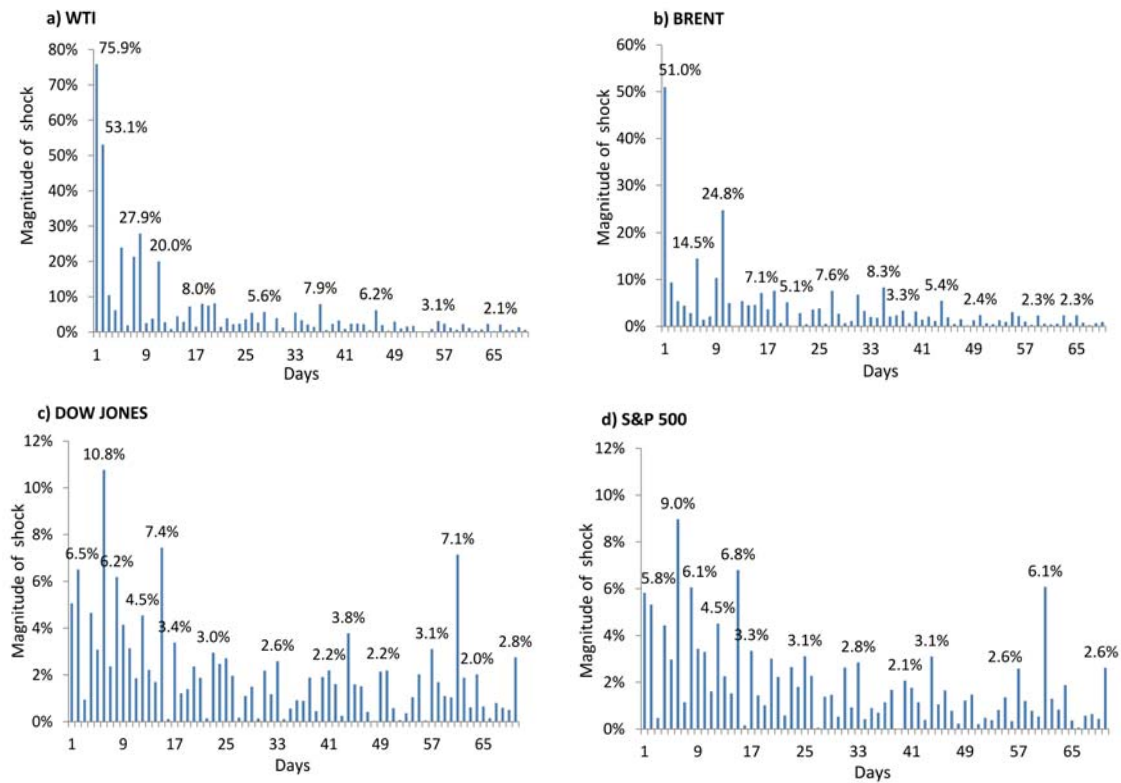


Figure 2. The aftershock sequences during the COVID-19 pandemic for the first 70 days (all shocks are in absolute values).

Table 1. Descriptive statistics for the periods under consideration and for the whole sample.

Sample	WTI OIL	BRENT OIL	DJIA	S&P 500
COVID-19 Period (for 70 days)				
Mean	0.9%	2.9%	0.5%	0.5%
Maximum	53.1%	51.0%	10.8%	9.0%
Minimum	−124.1%	−8.3%	−6.5%	−5.3%
Std. Dev.	18.9%	8.0%	2.9%	2.6%
Kurtosis	33.69	22.89	2.30	1.47
Skewness	−4.62	4.14	0.67	0.56
2008 period (for 70 days)				
Mean	−1.2%	0.1%	−0.1%	−0.2%
Maximum	10.8%	11.3%	10.3%	10.2%
Minimum	−12.0%	−10.7%	−8.2%	−9.5%
Std. Dev.	5.9%	4.5%	3.6%	3.9%
Kurtosis	0.80	−0.15	0.40	0.28
Skewness	0.75	0.14	0.12	−0.07
Total Sample				
Mean	−0.01%	0.06%	0.02%	0.02%
Maximum	53.1%	51.0%	10.8%	11.0%
Minimum	−302.0%	−47.5%	−13.8%	−12.8%
Std. Dev.	5.2%	2.6%	1.2%	1.2%
Kurtosis	2147.4	56.8	13.1	11.0
Skewness	−37.98	0.54	−0.38	−0.40

**Table 2.** Properties of the mainshock. Date, magnitude, standard deviation and relative shocks for the two crises.

Index	Date	Mainshock (%)	Sample Standard Deviation	Relative Shock
COVID-19 period				
WTI OIL	20 April 2020	302.0%	5.2%	58.35
BRENT OIL	21 April 2020	47.5%	2.6%	18.07
DJIA	16 March 2020	13.8%	1.2%	11.62
S&P 500	16 March 2020	12.8%	1.2%	10.30
2008–2009 period				
WTI OIL	22 September 2008	17.8%	5.9%	3.04
BRENT OIL	2 January 2009	19.9%	4.5%	4.39
DJIA	13 October 2008	10.5%	3.6%	2.93
S&P 500	13 October 2008	11.0%	3.9%	2.81

## 4. Empirical Properties

### 4.1. The Aftershock Sequences

We selected a time period of 70 trading days immediately following the mainshock to accurately measure the ongoing relaxation process. These trading days are equivalent to approximately 2.5 months, and we trace the aftershock sequences immediately after the mainshock. For instance, in the case of the WTI oil, during the pandemic, we trace the aftershock sequence immediately after the occurrence of the mainshock on 20 April 2020. For all cases, Table 2 presents the mainshocks.

We quantitatively described the number of times that the price change in absolute terms exceeded a given threshold value during this nonstationary time period, using threshold levels of  $\lambda = 1\sigma$ ,  $1.5\sigma$  and  $2\sigma$ , which were calculated from the whole sample's standard deviations. We utilized the Eviews statistics package for the calculations and we then accumulated the aftershocks with absolute price changes exceeding these threshold values and used Equation (2) to calculate the nonlinear fit for all cases, obtaining the values of the  $p$  parameter. In all cases, we detected a nonstationary process and nonlinear activity, with the aftershock sequence well approximated by the power law and with the Omori law holding after crashes of a large magnitude in both the crude oil and stock exchange markets.

Figure 3 shows the cumulative number of aftershocks,  $N(t)$ , for both the COVID-19 and Great Recession crises, compared to the best fit of Equation (2) for  $\lambda = 1\sigma$ ,  $1.5\sigma$  and  $2.0\sigma$ . During the COVID-19 period, the energy indices exhibited varying exponential  $p$ -values in the range of 0.86–1.96, but most values were close to 1. The WTI oil had greater  $p$ -values than Brent at all threshold values, indicating a faster relaxation process (faster decay) for the WTI, while Brent had a longer adjustment period.

Comparing the two major stock exchange indices, the relaxation values do not differ significantly and they vary with different thresholds, in the interval of 0.49–1.09. Table 3 summarizes all  $p$ -values for both the COVID-19 and the Great Recession aftershock sequences. The scaling values for the 2008 crisis are significantly smaller, signifying that the adjustment period towards the new equilibrium lasts longer. In addition, the relaxation exponent  $p$  increases when the threshold level  $\lambda$  increases from  $1.0\sigma$  to  $1.5\sigma$  to  $2.0\sigma$ , implying that larger aftershocks decay faster. In addition, as a quantitative measure of the goodness of fit, we present in Table 3 the root mean square of the residuals, indicated by the Greek character  $\chi$ . The root mean square (r.m.s.) for the basic estimated model is significantly smaller against the other estimated models (We also fit Equation (2) with two different specifications: the first by constraining the  $p$ -value between 0 and 1, i.e.,  $0 < p < 1$ , and the second by posing  $\tau = 0$ . In both of these alternative models, the r.m.s. is significantly larger than in the basic model).

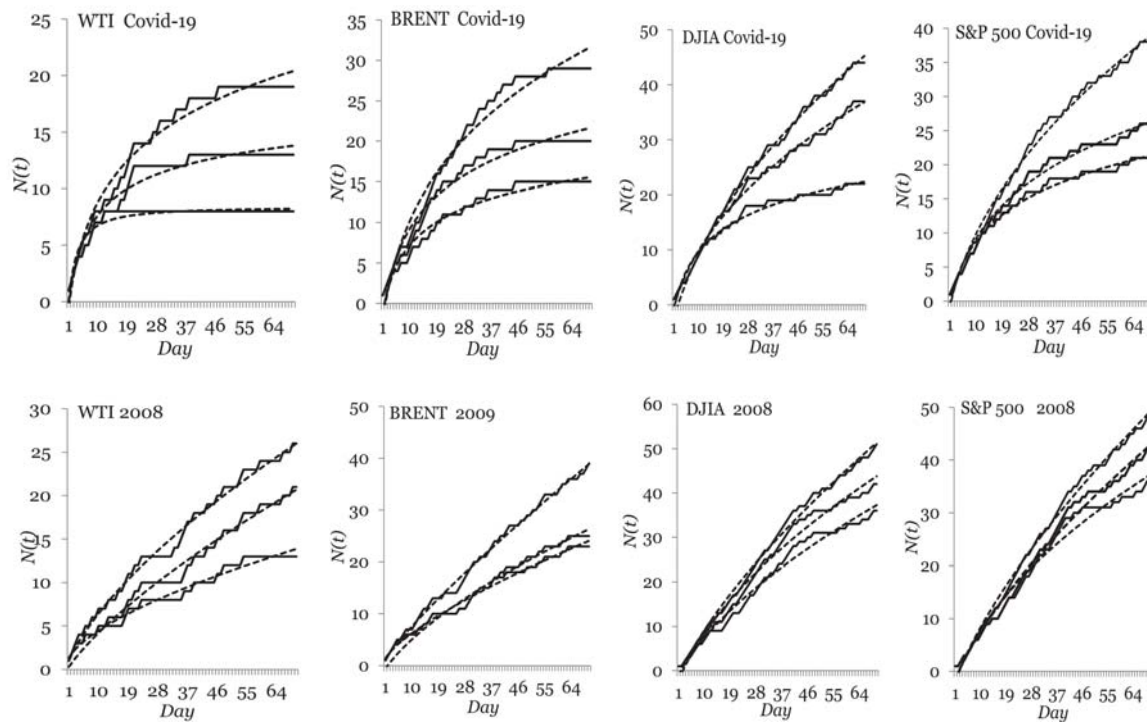


**Figure 3.** The cumulative number  $N(t)$  of aftershocks exceeding the threshold  $\lambda$  for the next 70 trading days after the mainshock. The dashed lines represent the best fit of Equation (2). In each graph, the curves from top to bottom represent the values exceeding the threshold levels set as  $\lambda = 1.0\sigma$ ,  $1.5\sigma$  and  $2.0\sigma$ . The first row of graphs depicts the COVID-19 crisis, while the second row represents the 2008–2009 crisis.

**Table 3.** Quantifying the Omori law. Scaling exponent  $p$  for all aftershock sequences and threshold values. The exponent values are for both the actual and shuffled data. The r.m.s. values of the fitting residuals are denoted by  $\chi$ .

Actual Data Index	$p$			$\chi$			Shuffled Data $p$		
	$1\sigma$	$1.5\sigma$	$2\sigma$	$1\sigma$	$1.5\sigma$	$2\sigma$	$1\sigma$	$1.5\sigma$	$2\sigma$
2020									
WTI	1.01	1.34	1.96	0.53	0.15	0.15	0.07	0.13	0.09
BRENT	0.82	1.07	1.16	2.00	1.14	0.56	0.08	0.11	0.00
DOW JONES	0.49	0.77	1.06	0.80	0.59	0.58	0.07	0.00	0.00
S&P 500	0.54	0.85	0.98	0.83	0.66	0.35	0.00	0.00	0.00
2008									
WTI	0.35	0.33	0.37	0.46	0.71	0.30	−0.06	0.06	0.01
BRENT	0.26	0.48	0.60	0.68	0.87	0.71	−0.03	0.05	0.09
DOW JONES	0.32	0.45	0.40	1.18	2.61	2.13	0.02	−0.07	0.01
S&P 500	0.33	0.35	0.51	0.96	1.46	1.54	0.02	0.06	0.02

Next, we investigate the role of random fluctuations by shuffling the aftershocks to remove correlations. We implement least square fits based on Equation (2) to obtain the scaling parameter  $p$ . In Figure 4, we present the scaling parameter  $p$  for all shuffled prices. Most of the values are close to zero, suggesting that the stochastic processes have no memory. For all different threshold values,  $\lambda$ , the random aftershock sequence  $N(t)$  exhibits linearity, indicating that the cumulative number  $N(t)$  increases linearly over time. Therefore, shuffling the data suggests that uncorrelated time series follow a Poisson distribution, as  $\log f(y) \sim -y$ .

In summary, it is evident that the value of the relaxation parameter  $p$  increases as the threshold value increases. Figure 5 presents the relaxation parameter for all cases, showing



that the crude oil aftershocks decay faster than the stock exchange prices, especially during the COVID-19 period.

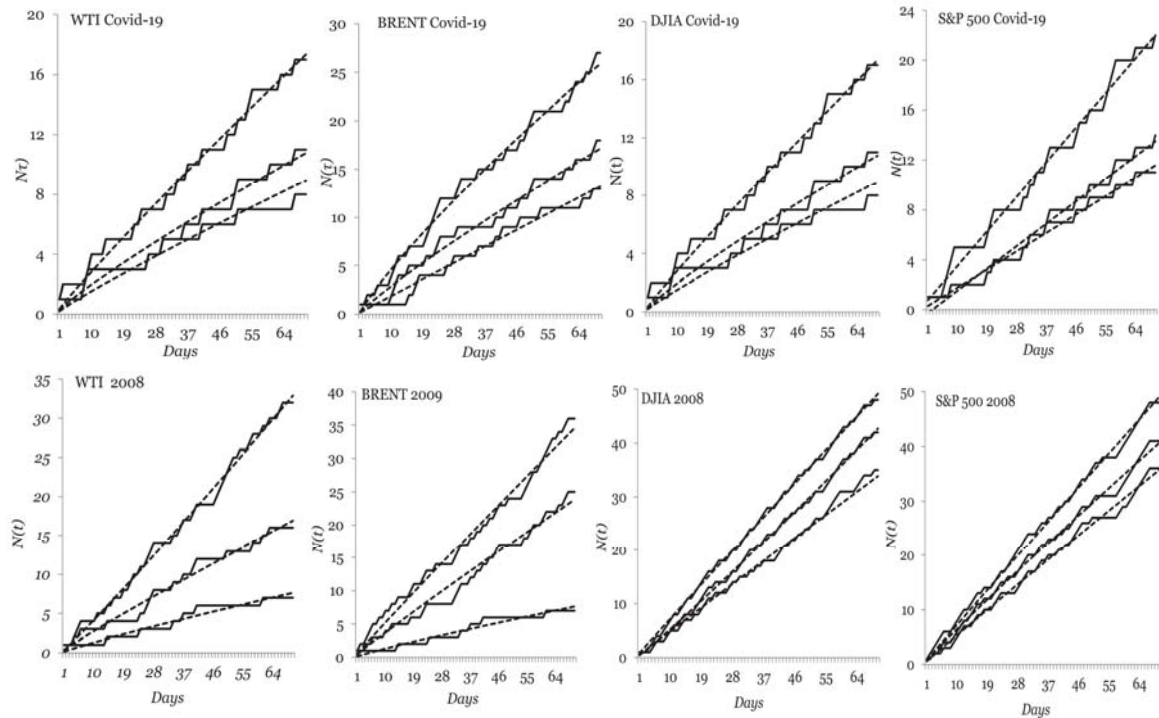


**Figure 4.** Cumulative number  $N(t)$  of aftershocks exceeding the threshold  $\lambda$  after shuffling the data. Dashed lines represent the best fit of Equation (2). Each graph displays curves with values exceeding the threshold levels of  $\lambda = 1.0\sigma$ ,  $1.5\sigma$  and  $2.0\sigma$  from top to bottom. The first row of graphs depicts the COVID-19 crisis, and the second row shows the 2008–2009 crisis. The period analyzed is 70 business days immediately after the occurrence of the mainshock.

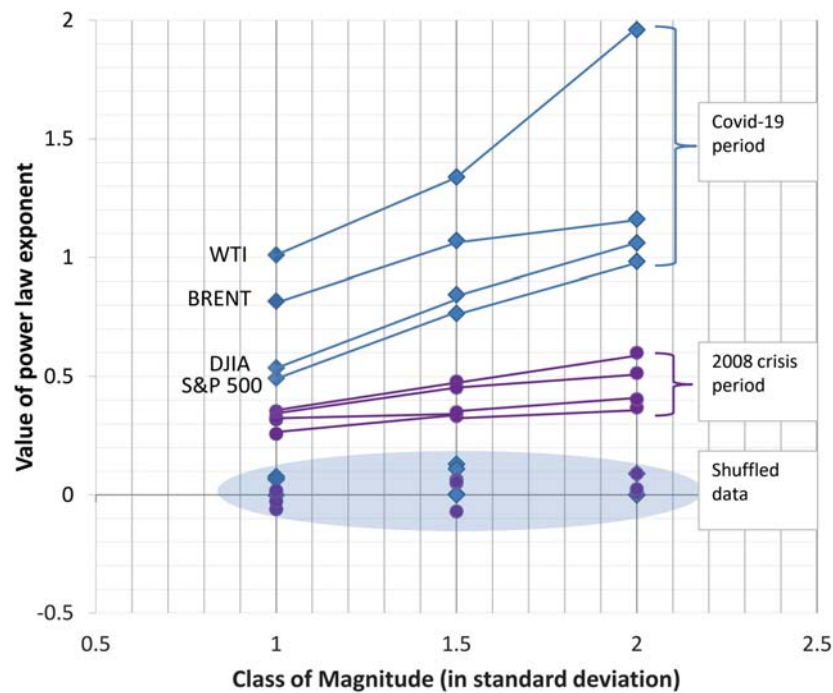


**Figure 5.** All scaling parameters for the COVID-19 and 2008–2009 crises. The dots represent various values with thresholds set (from left to right) at  $\lambda = 1\sigma$ ,  $1.5\sigma$  and  $2.0\sigma$ .

4.2. The Relation between the Mainshock and the Largest Shock in the Aftershock Sequence

In the preceding sections, we have described the properties of the aftershock sequences. However, there is a relationship between the aftershock sequence and the mainshock. It has been revealed, at least in the empirics of seismology, that there is a relation between the mainshock and the largest aftershock, known as Bath’s law [47] (Bath, 1965). In geophysics, the difference between these two shocks is approximately equal to 1.2, and the relation between them is given by the following equation:

$$D = M_0 - M_1 = 1.2 \tag{5}$$

where  $D$  is the difference between  $M_0 =$  mainshock and  $M_1 =$  largest aftershock.

Following [27] (Petersen et al., 2010), we conducted an analysis of the WTI and S&P 500, which are representative of the commodities and stock markets. We compared all mainshocks (shocks that were at least two standard deviations above the sample mean) to the largest aftershock in the aftershock sequence from January 2000 to February 2022. Our aftershock period window was set to five days immediately after the mainshock occurred. All price changes were measured in absolute values, and the parameter  $D$  was quantified according to Bath’s law.

$$M_0 - M_1 = \log_{10}M_0 - \log_{10}M_1 = D \tag{6}$$

Meanwhile, in functional formation, it is given as  $M_1/M_0 = C_D$ , where  $D = -\log_{10}C_D$ .

Figure 6 presents the linear relations among  $M_1/M_0$  for the WTI and S&P 500 and corresponds to  $D = -\log_{10}(C_D)$ ; for the WTI, it is  $D = -\log_{10}(0.548) = 0.261$ , while, for the S&P 500,  $D = -\log_{10}(0.609) = 0.215$ . In addition, the correlation coefficient for the WTI between the mainshocks and the second largest aftershock is  $r = 0.83$ ; for the S&P 500 case, it is  $r = 0.71$ . These results are in line with the ones obtained by [27] Petersen et al. (2010), but they are much smaller in magnitude than the 1.2 value obtained in geophysics.

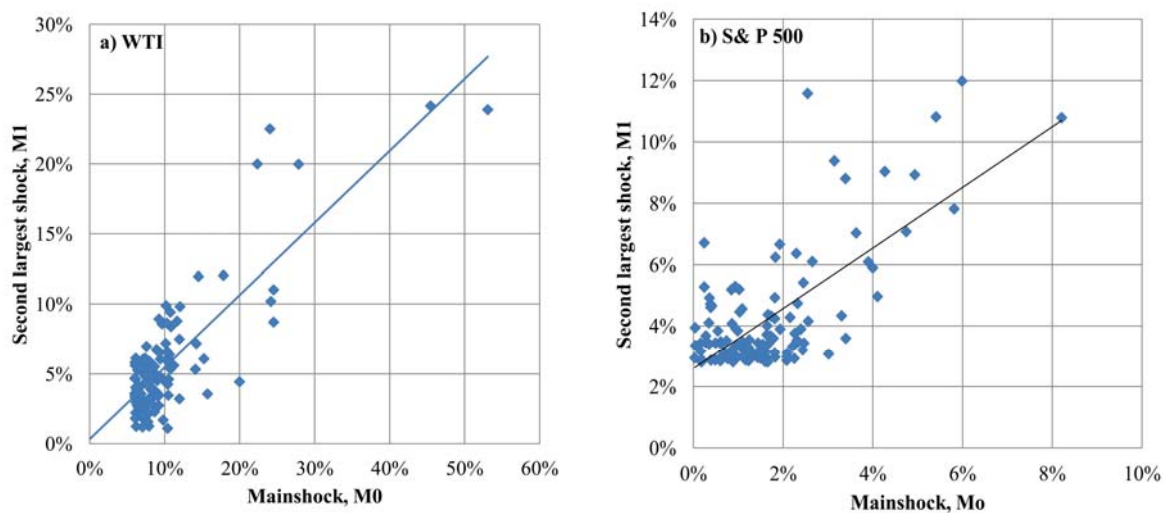


**Figure 6.** The relation between the size of the mainshock  $M_0$  and the size of the second largest aftershock  $M_1$  for the sample spanning from January 2000 until February 2022. Panel (a) shows the increasing relation for the WTI and panel (b) for S&P 500.

5. Policy Implications

This work represents the first effort to use power law modeling to explain how the oil prices behaved immediately following the greater-in-magnitude shock during the recent epidemic. Our research provides insights into how oil prices respond to significant disruptions in the financial markets, such the COVID-19 pandemic or the Great Recession. We found that the WTI oil prices were more volatile than the Brent oil prices during the

COVID-19 crisis, showing larger relaxation values at all threshold levels. This suggests that larger aftershocks decay faster and that the WTI's period of volatility is shorter than Brent's and the stock market indices'. Despite the fact that our data frequency was measured in days rather than minutes, this study's results are consistent with those obtained by [2] Lillo and Mantegna (2003), [6] Weber et al. (2007) and [27] Petersen et al. (2010), who tested the Omori law dynamics in stock exchange behavior. We depart from [26] Mu and Zhu's (2008) findings, especially with regard to the parameter  $p$ 's size, since they consistently reported values that were considerably greater than one ( $p > 1$ ). "The idiosyncratic microstructure of the Chinese stock market and/or the heavy influence of government intervention on the market" are likely the causes of the value discrepancy. Moreover, in line with the results derived by [27] Petersen et al. (2010), the use of the Bath law provides a conditional expectation of the largest aftershock, knowing the size of the mainshock.

Our findings provide significant information about the spatial distribution, the decay speed and the number of aftershocks. These elements are crucial and could be significant for risk estimation and forecasting purposes. Once the mainshock is known, we can predict the rate of aftershock occurrence using the Omori law technique; furthermore, knowing the characteristics of the Omori reaction might help in predicting the window of time within which aftershocks are likely to occur.

## 6. Conclusions

The utilization of Omori-law-based indicators for the prediction of financial crises and uncertainty provides a key foundation. Our findings and the estimation of the relaxation parameter for both the oil and stock markets confirm that the Omori law accurately demonstrates the nonstationary temporal variation in aftershock activity and shares similar perturbation response dynamics with earthquake studies. The concept of the Omori law offers a significant framework to model extreme events and uncertainty. During the COVID-19 crisis, the WTI oil prices exhibited greater volatility compared to the Brent oil prices, with higher relaxation values at all threshold levels. This indicates that larger aftershocks decay more rapidly, and the period of turbulence for the WTI is shorter than that of Brent and the stock market indices. As a robust measure, we shuffled the aftershock data for all prices and indices to determine whether the power law would hold. We found that linear behavior existed at all values of the threshold chosen.

When comparing the energy and stock markets, the mainshocks in the energy market, along with the variability and relaxation values, appear to be much greater than those in the stock exchange markets. The statistical regularity of the energy market's behavior, particularly immediately after the mainshock, provides valuable information for market participants, especially regarding expectations of the aftershock sequence. In other words, the response dynamics of the Omori sequence offer a timeframe within which aftershocks can be anticipated.

The assessment of only two extreme events for the oil market represents this study's shortcoming. Further research into more extreme events and a comparison of the Omori processes with alternative advanced machine- or deep-learning-based models are considered necessary.

This research can be further improved by employing higher-frequency data to test whether the relaxation dynamics still hold and whether Omori processes are induced by smaller-scale shocks, called subcrashes. In addition, future studies should focus on compiling a catalog of historical extreme events with great-magnitude shocks (market crashes), with the goal of determining the mean parameter value.

**Funding:** This research received no external funding.

**Data Availability Statement:** The data will be made available by the authors on request.

**Conflicts of Interest:** The author declares no conflict of interest.

## References

- Johansen, A.; Sornette, D. A hierarchical model of financial crashes. *Phys. A* **1998**, *261*, 581–598.
- Lillo, F.; Mantegna, N.R. Power-law relaxation in a complex system: Omori law after a financial crash. *Phys. Rev. E* **2003**, *68*, 016119. [[CrossRef](#)] [[PubMed](#)]
- Omori, F. On the aftershocks of earthquake. *J. Coll. Sci. Imp. Univ. Tokyo* **1894**, *7*, 111.
- Gabaix, X. Power Laws in Economics & Finance. *Annu. Rev. Econ.* **2009**, *1*, 255–294.
- Selcuk, F. Financial earthquakes, aftershocks and scaling in emerging stock markets. *Phys. A* **2004**, *333*, 306–316. [[CrossRef](#)]
- Weber, P.; Wang, F.; Vodenska-Chitkushev, I.; Havlin, S.; Stanley, E.H. Relation between volatility correlations in financial markets and Omori processes occurring on all scales. *Phys. Rev. E* **2007**, *76*, 016109. [[CrossRef](#)]
- Strogatz, S.H. Exploring complex networks. *Nature* **2001**, *410*, 268. [[CrossRef](#)]
- Focardi, S.; Cincotti, S.; Marchesi, M. Self-organization and market crashes. *J. Econ. Behav. Organ.* **2002**, *49*, 241–267. [[CrossRef](#)]
- Cont, R.; Bouchaud, J. Herd behaviour and aggregate fluctuations of financial markets. *Macroecon. Dyn.* **2000**, *4*, 170–196. [[CrossRef](#)]
- Stauffer, D.; Sornette, D. Self organized percolation model for stock market fluctuations. *Phys. A* **1999**, *271*, 496–506. [[CrossRef](#)]
- Levy, M.; Levy, H.; Solomon, S. A microscopic model of the stock market-cycles, booms and crashes. *Econ. Lett.* **1995**, *45*, 103–111. [[CrossRef](#)]
- Gabaix, X.; Parameswaran Gopikrishnan Plerou, V.; Stanley, H.E. A Theory of Power Law Distributions in Financial Market Fluctuations. *Nature* **2003**, *423*, 267–270. [[CrossRef](#)] [[PubMed](#)]
- Gabaix, X. Power Laws in Economics: An Introduction. *J. Econ. Perspect.* **2016**, *30*, 185–206. [[CrossRef](#)]
- Newman, M.E. Power laws, Pareto distributions and Zipf's law. *Contemp. Phys.* **2005**, *46*, 323–351. [[CrossRef](#)]
- Abe, S.; Suzuki, N.; Tayurskii, D. Aftershocks and Fluctuating Diffusivity. *Entropy* **2023**, *25*, 989. [[CrossRef](#)]
- Zavjalov, A.; Zotov, O.; Guglielmi, A.; Klain, B. On the Omori Law in the Physics of Earthquakes. *Appl. Sci.* **2022**, *12*, 9965. [[CrossRef](#)]
- Gupta, H.; Rekapalli, P.  $M_w \geq 5$  aftershocks of the 2008 Sichuan earthquake: Analysis of temporal variation of Omori Law  $p$ -value. *Front. Earth Sci.* **2022**, *10*, 964245. [[CrossRef](#)]
- Ommi, S.; Janalipour, M. Selection of shelters after earthquake using probabilistic seismic aftershock hazard analysis and remote sensing. *Nat. Hazards* **2022**, *113*, 345–363. [[CrossRef](#)]
- Zhang, Y.; Fan, J.; Marzocchi, W.; Shapira, A.; Hofstetter, R.; Havlin, S.; Ashkenazy, Y. Scaling laws in earthquake memory for interevent times and distances. *Phys. Rev. Res.* **2020**, *2*, 013264. [[CrossRef](#)]
- Im, K.; Avouac, J. Cascading foreshocks, aftershocks and earthquake swarms in a discrete fault network. *Geophys. J. Int.* **2023**, *235*, 831–852. [[CrossRef](#)]
- Siokis, M.F. Stock market dynamics: Before and after stock market crashes. *Phys. A Stat. Mech. Its Appl.* **2012**, *391*, 1315–1322. [[CrossRef](#)]
- Vallianatos, F. Gutenberg-Richter, Omori and Cumulative Benioff strain patterns in view of Tsallis entropy and Beck-Cohen Superstatistics. In Proceedings of the EGU General Assembly, Vienna, Austria, 24–28 April 2023. EGU23-5021.
- Zaccagnino, D.; Telesca, L.; Doglioni, C. Scaling properties of seismicity and faulting. *Earth Planet. Sci. Lett.* **2022**, *584*, 117511. [[CrossRef](#)]
- Sornette, D.; Johansen, A.; Bouchaud, J.-P. Stock market crashes, precursors and replicas. *J. Phys. I* **1996**, *6*, 167–175. [[CrossRef](#)]
- Di Matteo, T.; Aste, T.; Dacorogna, M. Scaling behaviors in differently developed markets. *Phys. A* **2003**, *324*, 183–188. [[CrossRef](#)]
- Mu, G.-H.; Zhou, W.-X. Relaxation dynamics of aftershocks after large volatility shocks in the SSEC index. *Phys. A Stat. Mech. Its Appl.* **2008**, *387*, 5211–5218. [[CrossRef](#)]
- Petersen, A.; Wang, F.; Havlin, S.; Stanley, H.E. Market dynamics immediately before and after financial shocks: Quantifying the Omori, productivity, and Bath laws. *Phys. Rev. E* **2010**, *82*, 036114. [[CrossRef](#)]
- Siokis, F. The dynamics of a complex system: The exchange rate crisis in Southeast Asia. *Econ. Lett.* **2012**, *114*, 98–101. [[CrossRef](#)]
- Pagnottoni, P.; Spelta, A.; Pecora, N.; Flori, A.; Pammolli, F. Financial earthquakes: SARS-CoV-2 news shock propagation in stock and sovereign bond markets. *Phys. A Stat. Mech. Its Appl.* **2021**, *582*, 126240. [[CrossRef](#)]
- Spelta, A.; Pecora, N.; Flori, A.; Giudici, P. The impact of the SARS-CoV-2 pandemic on financial markets: A seismologic approach. *Ann. Oper. Res.* **2021**, *330*, 639–664. [[CrossRef](#)]
- Rai, A.; Mahata, A.; Nurujjaman, M.; Prakash, O. Statistical properties of the aftershocks of stock market crashes revisited: Analysis based on the 1987 crash, financial-crisis-2008 and COVID-19 pandemic. *Int. J. Mod. Phys.* **2022**, *33*, 2250019. [[CrossRef](#)]
- Sun, X.; Yuan, O.; Xu, Z.; Yin, Y.; Liu, Q.; Wu, L. Did Zipf's Law hold for Chinese cities and why? Evidence from multi-source data. *Land Use Policy* **2021**, *106*, 105460. [[CrossRef](#)]
- Ning, Y.; Liu, S.; Zhao, S.; Liu, M.; Gao, H.; Gong, P. Urban growth rates, trajectories, and multi-dimensional disparities in China. *Cities* **2022**, *126*, 103717. [[CrossRef](#)]
- Ma, D.; Guo, R.; Jing, Y.; Zheng, Y.; Zhao, Z.; Yang, J. Intra-Urban Scaling Properties Examined by Automatically Extracted City Hotspots from Street Data and Nighttime Light Imagery. *Remote Sens.* **2021**, *13*, 1322. [[CrossRef](#)]
- Kopczewska, K.; Kopczewski, T. Natural spatial pattern—When mutual socio-geo distances between cities follow Benford's law. *PLoS ONE* **2022**, *17*, e0276450. [[CrossRef](#)]

36. Capello, R.; Caragliu, A.; Gerritse, M. Continuous vs. Discrete Urban Ranks: Explaining the Evolution in the Italian Urban Hierarchy over Five Decades. *Econ. Geogr.* **2022**, *98*, 438–463. [CrossRef]
37. Li, X.; Zhou, Y.; Gong, P. Diversity in global urban sprawl patterns revealed by Zipfian dynamics. *Remote Sens. Lett.* **2023**, *14*, 565–575. [CrossRef]
38. Najafi, A.; Darooneh, A.; Gheibi, A.; Farhang, N. Solar Flare Modified Complex Network. *Astrophys. J.* **2020**, *894*, 66. [CrossRef]
39. Kennedy, A.P.; Yam, C. On the authenticity of COVID-19 case figures. *PLoS ONE* **2020**, *15*, e0243123. [CrossRef]
40. Casals, B.; Salje, H.K. Energy exponents of avalanches and Hausdorff dimensions of collapse patterns. *Phys. Rev. E* **2021**, *104*, 054138. [CrossRef]
41. Abe, S.; Suzuki, N. Omori's law in the Internet traffic. *Europhys. Lett.* **2003**, *61*, 6. [CrossRef]
42. Wang, L.; Cao, S.; Jiang, X.; Salje, K.H.E. Cracking of human teeth: An avalanche and acoustic emission study. *J. Mech. Behav. Biomed. Mater.* **2021**, *122*, 104666. [CrossRef] [PubMed]
43. Chen, Y.; Tang, K.; Gou, B.; Jiang, F.; Ding, X.; Salje, K.H.E. Acoustic emission spectra and statistics of dislocation movements in Fe40Mn40Co10Cr10 high entropy alloys. *J. Appl. Phys.* **2022**, *132*, 080901. [CrossRef]
44. Utsu, T. A statistical study on the occurrence of aftershocks. *Geophys. Mag.* **1961**, *30*, 521–605.
45. Utsu, T. Aftershocks and Earthquake Statistics—Some Parameters Which Characterize an Aftershock Sequence and Their Interrelations. *J. Fac. Sci. Hokkaido Univ. Ser. 7 Geophys.* **1969**, *3*, 129–195.
46. U.S. Energy Information Administration. Petroleum Prices, Spot Prices. 2023. Available online: <https://www.eia.gov/opendata/browser/petroleum/pri/spt> (accessed on 1 September 2024).
47. Bath, M. Lateral inhomogeneities in the upper mantle. *Tectonophysics* **1965**, *2*, 483–514. [CrossRef]

**Disclaimer/Publisher's Note:** The statements, opinions and data contained in all publications are solely those of the individual author(s) and contributor(s) and not of MDPI and/or the editor(s). MDPI and/or the editor(s) disclaim responsibility for any injury to people or property resulting from any ideas, methods, instructions or products referred to in the content.